

Mass measurements on stable nuclides in the rare-earth region with the Penning-trap mass spectrometer TRIGA-TRAP

J. Ketelaer,^{1,2,*} G. Audi,³ T. Beyer,^{1,4} K. Blaum,^{1,4} M. Block,⁵ R. B. Cakirli,^{1,6} R. F. Casten,⁷ C. Droese,⁸ M. Dworschak,⁵ K. Eberhardt,⁹ M. Eibach,^{4,9} F. Herfurth,⁵ E. Minaya Ramirez,^{5,10} Sz. Nagy,^{1,5} D. Neidherr,^{1,10} W. Nörtershäuser,^{5,9} C. Smorra,^{4,9} and M. Wang^{3,11}

¹Max-Planck-Institut für Kernphysik, D-69117 Heidelberg, Germany

²Institut für Physik, Johannes Gutenberg-Universität, D-55128 Mainz, Germany

³CSNSM-IN2P3-CNRS, Université de Paris Sud, F-91405 Orsay, France

⁴Ruprecht-Karls-Universität, D-69120 Heidelberg, Germany

⁵GSI Helmholtzzentrum für Schwerionenforschung GmbH, D-64291 Darmstadt, Germany

⁶Department of Physics, University of Istanbul, Istanbul, Turkey

⁷Yale University, New Haven, Connecticut 06520-8120, USA

⁸Ernst-Moritz-Arndt-Universität, D-17487 Greifswald, Germany

⁹Institut für Kernchemie, Johannes Gutenberg-Universität, D-55128 Mainz, Germany

¹⁰Helmholtz-Institut Mainz, Johannes Gutenberg-Universität, D-55099 Mainz, Germany

¹¹Institute of Modern Physics, 730000 Lanzhou, China

(Received 16 November 2010; revised manuscript received 7 February 2011; published 12 July 2011)

The masses of 15 stable nuclides in the rare-earth region have been measured with the Penning-trap mass spectrometer TRIGA-TRAP. This is the first series of absolute mass measurements linking these nuclides to the atomic-mass standard ^{12}C . Previously, nuclear reaction studies almost exclusively determined the literature values of these masses in the Atomic-Mass Evaluation. The TRIGA-TRAP results show deviations on the order of 3–4 standard deviations from the latest published values of the Atomic-Mass Evaluation 2003 for some cases. However, the binding-energy differences that are important for nuclear structure studies have been confirmed and improved. The new masses are discussed in the context of valence proton-neutron interactions using double differences of binding energies, $\delta V_{pn}(Z, N)$.

DOI: [10.1103/PhysRevC.84.014311](https://doi.org/10.1103/PhysRevC.84.014311)

PACS number(s): 21.10.Dr, 07.75.+h, 27.70.+q, 32.10.Bi

I. INTRODUCTION

The evolution of nuclear structure often expresses itself through effects in quantities that are computable from nuclear masses, such as the sudden drop in two-neutron separation energies as a function of the neutron number in the case of shell closures. This stresses the need for high-precision mass measurements for nuclear structure studies as they are performed, e.g., using stored ions in Penning traps [1] or storage rings [2]. Within this work, the focus of Penning-trap mass measurements using the TRIGA-TRAP spectrometer [3] has been set on the stable isotopes of the elements europium, gadolinium, lutetium, and hafnium. The first two cover a transitional region around $N \approx 90$ [4], and the last two represent well-deformed, highly collective nuclei, where structure and binding energies are strongly linked [5]. Prior to the measurements reported here, the literature values of the masses in the rare-earth region in the Atomic-Mass Evaluation 2003 (AME 2003) [6,7], given in Table I, were determined by nuclear reaction studies, mainly of the (n, γ) type, with only a few exceptions. To this end, TRIGA-TRAP provides the first systematic series of direct mass measurements linking several stable nuclides in the rare-earth region to the atomic-mass standard ^{12}C . Furthermore, the results reported here test the present AME 2003 mass values independently from nuclear

reaction studies. The data have been implemented into the framework of the AME leading to new recommended mass values, as given in Table I, which can be used to study nuclear structure effects through the single and double differences of binding energies $B(Z, N) = [Zm_p + Nm_n - M(Z, N)]c^2$:

$$S_{2n}(Z, N) = B(Z, N) - B(Z, N - 2), \quad (1)$$

$$|\delta V_{pn}^{\text{ee}}| = \frac{1}{4}[\{B(Z, N) - B(Z, N - 2)\} - \{B(Z - 2, N) - B(Z - 2, N - 2)\}], \quad (2)$$

where $[m_p, m_n, M(Z, N)]$ denote the proton, neutron, and nuclear masses. Equation (2) expresses the average interaction between the last two protons and the last two neutrons [8,9] for even- Z and even- N nuclides. By using this relation and considering only the number of *valence* nucleons, an interesting effect is found in the region of rare-earth nuclides. It can be interpreted similarly to the Wigner energy, which is well known for light $N \simeq Z$ nuclei [10,11] and will be discussed in Sec. IV.

This paper shows the importance of direct mass measurements in the region around the stable rare-earth nuclides, since deviations of a few keV from the literature values have been found. However, the binding-energy differences that are important for nuclear structure studies, as derived from the AME 2003 values, using Eqs. (1) and (2), remain in general unaffected. Thus, they were confirmed and improved within this work.

*ketela@uni-mainz.de

TABLE I. Results of the mass measurements in the rare-earth region. The columns from left to right represent the element, the proton and neutron numbers, the investigated molecule ion, the reference ion, the number of individual measurements (No.), the mean frequency ratio r with the total uncertainty, the atomic mass of the nuclide, the relative mass uncertainty, the atomic-mass excess ME_{exp} obtained at TRIGA-TRAP, the literature value ME_{AME03} [7], and the new adjusted mass excess ME_{new} calculated by two of the co-authors (G.A., M.W.). Note that ME_{new} also includes other experimental data which has become available since the AME 2003 was published. Rows labeled with (*) contain accuracy checks with carbon clusters, where the mass excess values refer to the cluster and not to the ^{12}C atom. For details see text.

Element	Z	N	Ion	Refer.	No.	r	m (μu)	$\delta m/m$ (10^{-8})	ME_{exp} (keV)	ME_{AME03} (keV)	ME_{new} (keV)	
Eu	63	90	$^{153}\text{Eu}^{16}\text{O}^+$	$^{12}\text{C}_{14}^+$	2	1.0054532942(343)	152 921235.8(5.8)	3.77	-73368.4(5.4)	-73373.5(2.5)	-73366.4(1.7)	
			*	$^{12}\text{C}_{15}^+$	$^{12}\text{C}_{14}^+$	2	1.0714288017(371)			-0.5(5.8)	0(0)	
Gd	64	88	$^{152}\text{Gd}^{16}\text{O}^+$	$^{12}\text{C}_{14}^+$	4	0.9994923158(209)	151 919794.7(3.5)	2.31	-74710.8(3.3)	-74714.2(2.5)	-74706.6(1.5)	
			64	90	$^{154}\text{Gd}^{16}\text{O}^+$	$^{12}\text{C}_{15}^+$	3	0.9439764595(237)	153 920878.8(4.3)	2.77	-73700.9(4.0)	-73713.2(2.5)
	64	91	$^{155}\text{Gd}^{16}\text{O}^+$	$^{12}\text{C}_{15}^+$	4	0.9495417784(147)	154 922633.2(2.6)	1.71	-72066.7(2.5)	-72077.1(2.5)	-72069.5(1.5)	
	64	92	$^{156}\text{Gd}^{16}\text{O}^+$	$^{12}\text{C}_{15}^+$	4	0.9550946098(200)	155 922139.8(3.6)	2.31	-72526.3(3.4)	-72542.2(2.5)	-72534.6(1.5)	
	64	93	$^{157}\text{Gd}^{16}\text{O}^+$	$^{12}\text{C}_{15}^+$	3	0.9606603600(183)	156 923971.8(3.3)	2.10	-70819.9(3.1)	-70830.7(2.5)	-70823.1(1.5)	
	64	94	$^{158}\text{Gd}^{16}\text{O}^+$	$^{12}\text{C}_{14}^+$	1	1.0352324681(491)	157 924120.7(8.3)	5.22	-70681.1(7.7)			
			$^{158}\text{Gd}^{16}\text{O}^+$	$^{12}\text{C}_{15}^+$	3	0.9662167424(179)	157 924117.5(3.2)	2.04	-70684.1(3.0)			
			$^{158}\text{Gd}^{16}\text{O}^+$	average		157 924118.0(3.0)	1.90	-70683.7(2.8)	-70696.8(2.5)	-70689.1(1.5)		
	64	96	$^{160}\text{Gd}^{16}\text{O}^+$	$^{12}\text{C}_{15}^+$	4	0.9773442650(199)	159 927065.5(3.6)	2.24	-67938.0(3.3)	-67948.6(2.6)	-67941.1(1.6)	
	*			$^{12}\text{C}_{14}^+$	$^{12}\text{C}_{15}^+$	4	0.9333331419(148)			2.0(2.5)	0(0)	
*			$^{12}\text{C}_{15}^+$	$^{12}\text{C}_{14}^+$	3	1.0714287811(277)			-3.7(4.3)	0(0)		
*			$^{12}\text{C}_{16}^+$	$^{12}\text{C}_{15}^+$	4	1.0666668629(216)			-1.2(3.6)	0(0)		
Lu	71	104	$^{175}\text{Lu}^{16}\text{O}^+$	$^{12}\text{C}_{16}^+$	4	0.9944566701(234)	174 940769.1(4.5)	2.57	-55173.2(4.2)	-55170.7(2.2)	-55167.1(1.9)	
			71	105	$^{176}\text{Lu}^{16}\text{O}^+$	$^{12}\text{C}_{16}^+$	3	0.9996750300(394)	175 942691.3(7.6)	4.30	-53382.7(7.1)	-53387.4(2.2)
	*			$^{12}\text{C}_{15}^+$	$^{12}\text{C}_{16}^+$	4	0.9374998460(217)			4.4(3.9)	0(0)	
Hf	72	104	$^{176}\text{Hf}^{16}\text{O}^+$	$^{12}\text{C}_{16}^+$	4	0.9996683922(511)	175 941416.9(9.8)	5.58	-54569.9(9.1)	-54577.5(2.2)	-54578.0(3.6)	
			72	105	$^{177}\text{Hf}^{16}\text{O}^+$	$^{12}\text{C}_{16}^+$	4	1.0048862367(375)	176 943240.1(7.2)	4.07	-52871.5(6.7)	-52889.6(2.1)
	72	106	$^{178}\text{Hf}^{16}\text{O}^+$	$^{12}\text{C}_{16}^+$	4	1.0100970872(413)	177 943720.6(7.9)	4.47	-52423.9(7.4)	-52444.3(2.1)	-52441.2(1.9)	
	72	107	$^{179}\text{Hf}^{16}\text{O}^+$	$^{12}\text{C}_{16}^+$	4	1.0153163888(336)	178 945823.6(6.5)	3.61	-50465.0(6.0)	-50471.9(2.1)	-50468.9(1.9)	
	72	108	$^{180}\text{Hf}^{16}\text{O}^+$	$^{12}\text{C}_{16}^+$	4	1.0205285770(340)	179 946560.9(6.5)	3.63	-49778.2(6.1)	-49788.4(2.1)	-49785.3(1.9)	
			*			$^{12}\text{C}_{15}^+$	$^{12}\text{C}_{16}^+$	4	0.9374998408(213)			3.5(3.8)

II. EXPERIMENTAL SETUP AND TECHNIQUE

The Penning-trap mass spectrometer TRIGA-TRAP is installed at the research reactor TRIGA Mainz as part of the TRIGA-SPEC project [3]. The experimental setup is shown in Fig. 1. For the measurements reported here, the nonresonant laser-ablation ion source described in detail in Ref. [12] has been used to produce the ions of interest, as well as carbon-cluster ions, as mass references. For this purpose, a frequency-doubled, pulsed Nd:YAG laser irradiates a Sigradur surface where the element under investigation has been deposited. Within the 7-T superconducting magnet, two Penning traps are located where the charged particles are stored in a superposition of the strong homogeneous magnetic field and a weak electrostatic quadrupole field. The ion motion inside a Penning trap is well understood [13]. It consists of two independent harmonic radial motions in the plane perpendicular to the magnetic field, i.e., the slow magnetron and the fast cyclotron motion, and a harmonic axial oscillation

along the field lines. The first trap (purification trap) has a cylindrical shape and is used to prepare the ion bunch by mass-selective buffer-gas cooling [14]. Afterwards, the nuclide of interest is transferred through a differential pumping channel [15] with 1.5 mm inner diameter to the hyperbolic precision trap, where the actual mass measurement takes place. This is done by determining the cyclotron frequency

$$\nu_c = \frac{1}{2\pi} \frac{q}{m} B \quad (3)$$

of an ion with charge-to-mass ratio q/m stored in a magnetic field with strength B , using the so-called time-of-flight-ion-cyclotron-resonance (TOF-ICR) technique [16,17]. Here the ions are excited by rf fields in the radial plane prior to the ejection toward an ion detector, i.e., Channeltron electron multiplier (CEM), at the end of the setup. The flight time between trap and detector is recorded as a function of the excitation frequency leading to a minimum in the case where

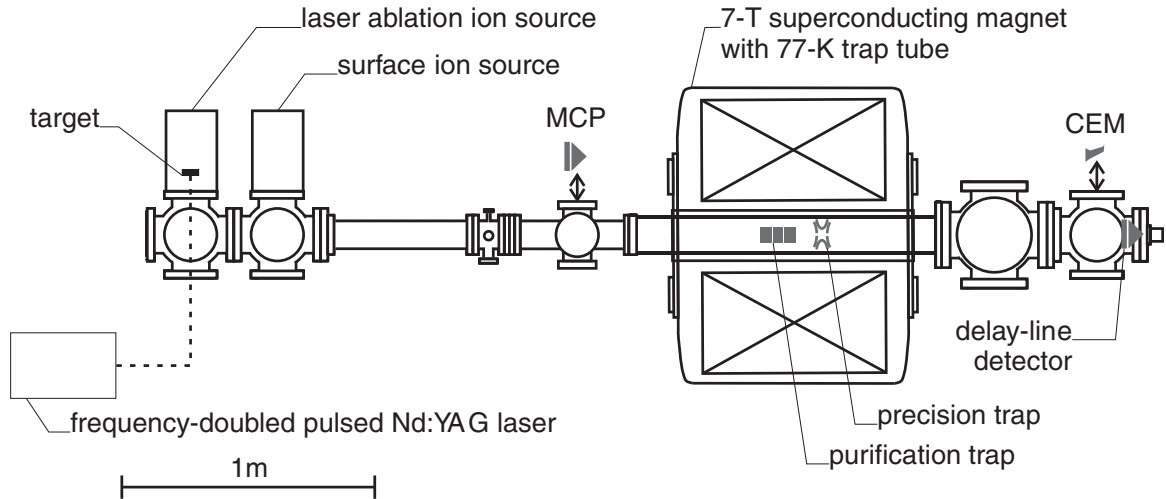


FIG. 1. (Color online) Top view of the TRIGA-TRAP setup. The two off-line ion sources are shown on the left, followed by the superconducting magnet with two Penning traps. The ion detector used in the TOF-ICR measurements is located on the right (CEM: Channeltron electron multiplier). Two other ion detectors (MCP: Microchannel plate; delay-line detector) can be used for beam monitoring. For details see text.

the applied rf field is in resonance at ν_c . Instead of a continuous excitation, the Ramsey method with two separated pulses is routinely applied at TRIGA-TRAP, since precision up to three times higher is gained without the need to increase the storage time [18]. The required calibration of the magnetic field [see Eq. (3)] is done performing a measurement with carbon-cluster reference ions of similar m/q before and after the measurement of the ion of interest, since their mass is known by definition besides the negligible contributions from cluster binding energies [19]. Both reference frequencies are used to interpolate to the time when the actual measurement took place. The data analysis procedure, as well as systematic accuracy studies, at TRIGA-TRAP are explained in detail in [20], leading to the frequency ratio of the single-charged ions,

$$r = \frac{\nu_{c,\text{ref}}}{\nu_c}, \quad (4)$$

between the cyclotron frequency of the reference ion $\nu_{c,\text{ref}}$ and the ion of interest ν_c . The mass of the neutral species can be calculated by

$$m = r(m_{\text{ref}} - m_e) + m_e, \quad (5)$$

where m_e is the electron mass. In nuclear physics, usually the mass excess

$$ME = (m - A \times u) c^2 \quad (6)$$

is referred to, rather than the mass itself.

III. MASS MEASUREMENTS AND RESULTS

The masses of 15 stable nuclides of the elements europium ($Z = 63$), gadolinium ($Z = 64$), lutetium ($Z = 71$), and hafnium ($Z = 72$) have been measured using the TOF-ICR technique, with a Ramsey excitation profile of two 100-ms pulses and an intermediate waiting time of 800 ms. The

targets for our laser ion source were produced by drying an acid solution of a natural admixture of the element under investigation on a Sigradur backing. In the case of ^{152}Gd with a natural abundance of only 0.20(1)% [21], a sample with about 35% enrichment was used. To avoid isobaric contaminations, separate targets have been prepared for each element. The atom density in the deposited layer was about 10^{14} – $10^{17}/\text{mm}^2$ in each case, leading to a count rate of up to 1 ion per laser pulse stored in the precision trap, using a laser intensity of about 100–500 $\mu\text{J}/\text{mm}^2$. In the mass measurements reported here, the corresponding single-charged monoxide ions were used since they yielded the largest count rate. Background ions with a mass difference of at least 15–20 u to the desired ions, mainly sodium, potassium, and certain carbon clusters, were blocked by a beam gate due to a different flight time. The preparation and selection of a single ion species after this preselection was done by mass-selective buffer-gas cooling in the purification trap with a resolving power of about 50 000. In a combinatorial analysis, all possible combinations of nuclides of typically present elements (e.g., H, He, C, N, O) creating contaminant molecules with a cyclotron frequency in a window of ± 5 Hz around the frequencies of interest could be discarded due to chemical or abundance reasons. Thus, contaminations were not an issue during the measurements reported here. An example TOF-ICR resonance obtained for $^{152}\text{Gd}^{16}\text{O}^+$ ions with the precision trap is shown in Fig. 2 together with a fit of the theoretical line shape of the Ramsey excitation pattern [22] yielding the cyclotron frequency. The results of all mass measurements are listed in Table I, separated into four packages corresponding to four experimental runs, with each investigating a single element. In addition, the results of cross-checks using carbon clusters are given, which have been performed to ensure the accuracy and to confirm the systematic studies reported in Ref. [20] for the individual runs separately. The corresponding data given in the rows labeled with an asterisk show that the measured mass excesses for

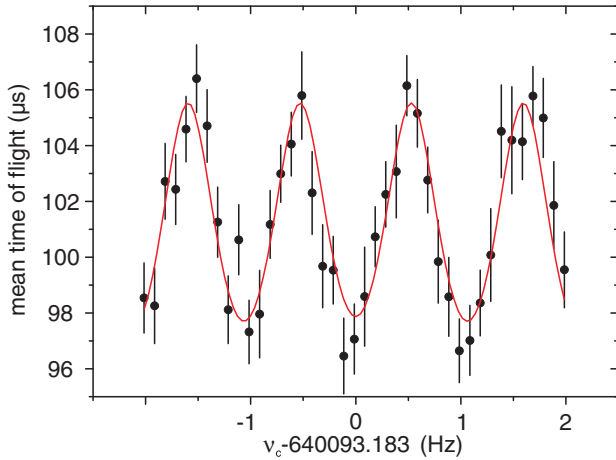


FIG. 2. (Color online) Time-of-flight resonance with 542 $^{152}\text{Gd}^{16}\text{O}^+$ ions in total, using a Ramsey excitation pattern [18,22] with two 100-ms pulses and an intermediate waiting time of 800 ms. The solid line is a fit of the theoretical line shape leading to the center frequency of $\nu_c = 640093.183(12)$ Hz.

carbon clusters agree well within the given uncertainties with the expected value of zero. Moreover, the reduced chi square

$$\chi_n^2 = \frac{1}{f} \sum_i \left[\frac{ME_i}{\delta ME_i} \right]^2, \quad (7)$$

with the experimental mass excesses $ME_i \pm \delta ME_i$, and the number of degrees of freedom f , is 0.9 for the set of all carbon-cluster cross-checks, which is well within the expectation range of 1 ± 0.25 . Contributions of binding energies to the cluster masses are on the order of 100 eV [23], thus they can be neglected at our level of precision. For each nuclide of interest, the ion species used in the mass measurement, the reference ion species, and the mean frequency ratio r obtained by the given number of individual measurements are listed. The contributions of magnetic field fluctuations of $6(2) \times 10^{-11}/\text{min} \times \Delta t$ per time interval Δt between the two calibration measurements are quadratically added to the distinct statistical uncertainties δr_i from the fits of the theoretical lines shapes. During the measurements reported here, the typical time interval was about three hours, leading to an uncertainty of 1×10^{-8} . Finally, a systematic shift of $-2.2(2) \times 10^{-9} \times (m - m_{\text{ref}})/u$, depending on the difference between the mass of interest and the reference mass, is corrected and the corresponding systematic uncertainty is considered [20]. For the cases of $^{154-157}\text{Gd}$, $^{12}\text{C}_{15}^+$ was chosen as the reference due to the larger production rate as compared to $^{12}\text{C}_{14}^+$ and since the mass-dependent systematic shift still did not limit the precision. The total uncertainty of r is given with three significant digits to allow for intermediate calculations in the AME 2003 with no loss of precision, and rounding being applied only at the final stage. Furthermore, the atomic masses of the nuclides of interest [see Eq. (5)] have been calculated subtracting the oxygen mass $m(^{16}\text{O}) = 15.99491461956(16)$ u [7] and neglecting the molecular binding energies of the oxide ions, which are on the order of eV. The resulting mass excesses [see Eq. (6)], ME_{exp} , are compared

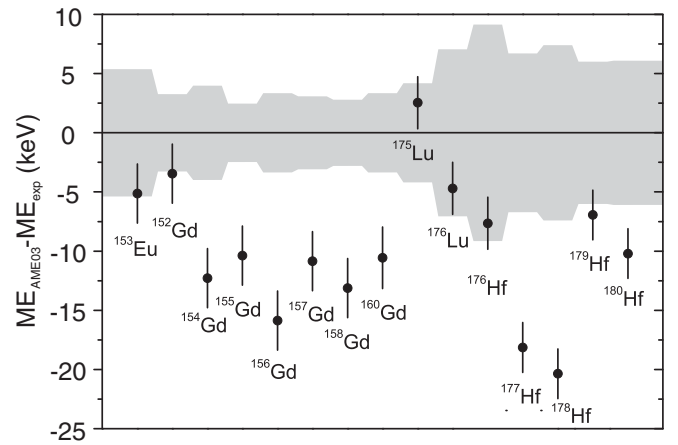


FIG. 3. Differences between the measured mass excesses ME_{exp} (zero line) and the literature values from the AME 2003, ME_{AME03} (black dots) [7]. One standard deviation is indicated by the gray band in the case of the TRIGA-TRAP values and by the error bars for the AME-2003 data. For details and discussion, see text.

to the latest published values taken from the AME 2003. The differences $ME_{\text{AME03}} - ME_{\text{exp}}$ are graphically displayed in Fig. 3, showing a general trend of the literature values to be too strongly bound by 5–20 keV. However, in the cases of ^{153}Eu , ^{152}Gd , $^{175,176}\text{Lu}$, and $^{176,179}\text{Hf}$, the results obtained at TRIGA-TRAP agree with the AME-2003 values. To provide a further confirmation, besides the carbon-cluster cross-checks listed in Table I, the SHIPTRAP facility (GSI, Darmstadt) [24] has been used. Within the studies reported here, the mass excess of ^{158}Gd has been measured there also, leading to $ME_{\text{SHIPTRAP}}(^{158}\text{Gd}) = -70\,687.7(7.4)$ keV. This is in excellent agreement with the TRIGA-TRAP measurement in Table I as well as the AME-2003 value, due to the large uncertainty of the SHIPTRAP value. In an earlier experiment at TRIGA-TRAP, the mass of ^{197}Au , which was already known to high precision, could be reproduced [20], serving as another accuracy test.

We would like to emphasize that the mass measurements reported here provide the first direct links between the nuclides under investigation and the atomic-mass standard ^{12}C . Moreover, the present AME-2003 values are tested independently from (n, γ) studies, which is certainly required, as the example of ^{32}Si shows. Here, a 4σ deviation of the mass value determined by a chain of (n, γ) reactions starting with ^{28}Si to the direct mass measurement has been discovered [25]. Regarding the nuclides investigated here, only ^{179}Hf had a direct connection to carbon in the AME framework, whereas (n, γ) reaction energies were the dominating ingredients in the mass adjustment. Those create, together with other inputs to the AME 2003 such as α , β^+ , and β^- decays and a few mass spectrometric relations, a complex network of strong correlations for the mass adjustment in the rare-earth region [7], involving the risk of a few wrong links affecting a complete subnetwork of nuclides. This might explain the discrepancies between the adjusted values published in the AME 2003 and the recent experimental results from TRIGA-TRAP. In order to take all connections into account, which usually

overdetermine the masses, the AME is based on a least-squares fit to the experimental data, described by a set of linear equations. Details about this treatment can be found in [6] and, especially concerning Penning-trap measurements, in [26,27]. Even though several results reported here agree with values from the mass tables as well as with recent measurements from mass spectrometry, and all the carbon-to-carbon cross-checks are compatible with a null difference, the fact that some of the TRIGA-TRAP data deviate significantly (see Fig. 3) triggered a further test. We performed a simulation where the TRIGA-TRAP results were considered to be exact, which allows one, in some simple cases, to locate the AME input data, which pulls the mass surface in a wrong direction. Since no clear evidence for one or a few outliers was found, more measurements have to be performed in the neighborhood, but also in other different regions of the nuclear chart. In this way, the possible outliers, which deformed the mass surface, should be delineated. In the following, the TRIGA-TRAP results are compared to other experimental results that have been considered in the AME 2003 in order to search for the origin of the discrepancies shown in Fig. 3.

A. ^{153}Eu

The TRIGA-TRAP result for ^{153}Eu is confirmed by a measurement with the Penning-trap mass spectrometer ISOLTRAP (CERN). Taking their published frequency ratio of 1.800 947 577(187) between $^{153}\text{Eu}^+$ and $^{85}\text{Rb}^+$ [26] results in an atomic mass of $m(^{153}\text{Eu}) = 152\,921\,242.6(15.9)\,\mu\text{u}$, which agrees with the present result in Table I but has about three times larger uncertainty. The AME-2003 value is determined by the nuclear reactions $^{152}\text{Eu}(n,\gamma)^{153}\text{Eu}$ [28] and $^{153}\text{Eu}(n,\gamma)^{154}\text{Eu}$ [29,30] relating the mass of ^{153}Eu to the masses of its neighboring isotopes by the neutron-separation energies. Figure 3 shows an agreement between the AME 2003 and the recent TRIGA-TRAP result. However, the AME-2003 uncertainty is about a factor of 2 smaller than the one reported here, due to the high precision of the reaction measurements.

B. $^{152,154-158,160}\text{Gd}$

In the AME 2003, the mass of ^{152}Gd has been determined by the neutron-separation energy from $^{152}\text{Gd}(n,\gamma)^{153}\text{Gd}$ averaged over two individual measurements [28,31]. The value is in agreement with the TRIGA-TRAP result (see Fig. 3). However, the measurement reported here was the first independent confirmation of the mass of ^{152}Gd by an entirely different technique, establishing a direct connection to ^{12}C . Thus, this isotope now changed its status in the AME adjustment from a so-called secondary to a primary nuclide [6].

The masses of the isotopes $^{154-158}\text{Gd}$ in the AME 2003 have also been mainly determined by (n,γ) measurements [28,30-35] and show discrepancies of 3-4 σ (standard deviations) to the TRIGA-TRAP results (see Fig. 3). In Fig. 4, for each gadolinium isotope, the neutron-separation energy S_n , averaged over all corresponding reaction studies used as input parameters in the AME 2003, is compared to the value calculated using the TRIGA-TRAP measurements from

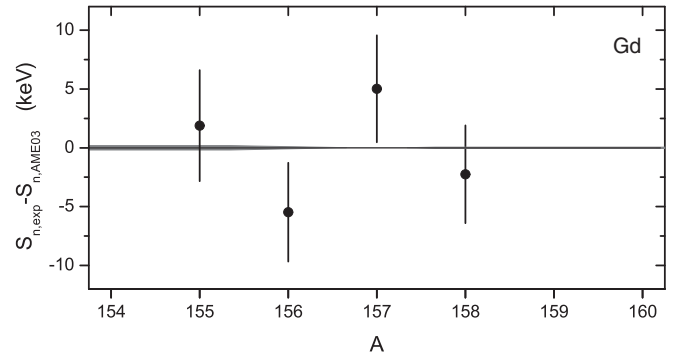


FIG. 4. Comparison between the neutron-separation energies S_n averaged over (n,γ) results used as input parameters in the AME 2003 $S_{n,\text{AME03}}$ [6] (zero line) to the values obtained through the TRIGA-TRAP measurements $S_{n,\text{exp}}$ (data points) for gadolinium isotopes. The error bars denote one standard deviation of the TRIGA-TRAP results and the gray band denotes the AME-2003 values.

Table I. The agreement is better than 1.3 σ . A direct mass measurement of ^{153}Gd is required to identify the origin of the disagreement between the deviations to the AME-2003 values of the masses of ^{152}Gd and heavier gadolinium isotopes either in the neutron-separation energy from $^{152}\text{Gd}(n,\gamma)^{153}\text{Gd}$ or from $^{153}\text{Gd}(n,\gamma)^{154}\text{Gd}$. Other significant contributions to certain gadolinium masses in the AME 2003 come from the decays $^{154,155}\text{Eu}(\beta^-)^{154,155}\text{Gd}$ (average Q value in [6]) and from the measurement $^{154}\text{Sm} - ^{154}\text{Gd}$ [36], which cannot be compared yet to the TRIGA-TRAP results (Table I) since additional masses would be needed.

For ^{160}Gd , the mass difference $m(^{160}\text{Gd}) - m(^{158}\text{Gd}) = 2\,002\,949.9(4)\,\mu\text{u}$, averaged over two mass spectrometric measurements [36,38] used in the AME-2003 adjustment, agrees with the TRIGA-TRAP result of $2\,002\,947.5(4.7)\,\mu\text{u}$. The AME-2003 value of the mass of ^{160}Gd is mainly determined by the $^{160}\text{Gd}(\alpha,t)^{161}\text{Tb}$ reaction [37], and the mass spectrometric doublets $^{160}\text{Gd}^{35}\text{Cl} - ^{158}\text{Gd}^{37}\text{Cl}$ [36,38] and $^{160}\text{Gd} - ^{160}\text{Dy}$ [39].

C. $^{175,176}\text{Lu}$

Both masses of the lutetium isotopes measured at TRIGA-TRAP conform with the AME values from 2003 (see Fig. 3). The neutron-separation energy of ^{176}Lu of 6280.8(8.2) keV, as extracted from the TRIGA-TRAP results, agrees well with the value of 6288.0(0.2) keV obtained by a $^{175}\text{Lu}(n,\gamma)^{176}\text{Lu}$ reaction measurement [40], contributing about 77% to the determination of the mass of ^{175}Lu and about 23% to the mass of ^{176}Lu in the AME 2003. A further quantity that can be compared to other experiments is the Q_{β^-} value of the decay $^{176}\text{Lu}(\beta^-)^{176}\text{Hf}$, which amounts to 1187.1(11.7) keV, using the TRIGA-TRAP results. A decay study of the 1^- isomeric state of $^{176\text{m}}\text{Lu}$ [41] gives $Q_{\beta^-} = 1194.1(1.0)$ keV after a later discovered correction of the corresponding excitation energy [40]. Further significant influences on the masses of $^{175,176}\text{Lu}$ within the AME-2003 adjustment are the studies of the decay $^{175}\text{Yb}(\beta^-)^{175}\text{Lu}$, the nuclear reaction $^{176}\text{Lu}(n,\gamma)^{177}\text{Lu}$ (average values for both items published in [6]), and the mass difference $^{176}\text{Lu}^{37}\text{Cl} - ^{143}\text{Nd}^{35}\text{Cl}_2$ [42].

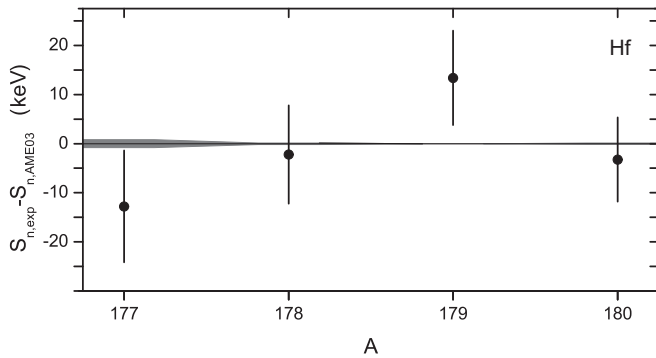


FIG. 5. Comparison between S_n of certain hafnium isotopes obtained from (n, γ) studies and the values calculated from the results within this work. For details, see Fig. 4 and text.

D. $^{176-180}\text{Hf}$

While there is a good agreement with the AME-2003 values for $^{176,179}\text{Hf}$, the TRIGA-TRAP result for ^{180}Hf shows an offset of 1.7σ . The discrepancy is even 2.7σ in the case of $^{177,178}\text{Hf}$. To investigate the origin of the discrepancies, a series of neutron-separation energies is calculated for the hafnium isotopes to be compared to the $^{176-179}\text{Hf}(n, \gamma)^{177-180}\text{Hf}$ measurements [30,43–46], which dominate the corresponding adjusted mass values in the AME 2003, which is similar to the case of gadolinium. They are presented in Fig. 5, showing an agreement for S_n of better than 1.5σ in all cases. However, mass measurements with a final uncertainty of less than $1 \text{ keV}/c^2$ would be needed in order to identify possible wrong (n, γ) results. The mass difference $m(^{180}\text{Hf}) - m(^{179}\text{Hf}) = 1\,000\,730.8(4.7) \mu\text{u}$ [47] measured in a magnetic mass spectrometer agrees with the TRIGA-TRAP result of $1\,000\,737.3(9.2) \mu\text{u}$. Furthermore, a measurement linking the hafnium isotope ^{179}Hf to the atomic-mass standard ^{12}C is used as an input in the AME 2003, which is the isobaric mass doublet $^{12}\text{C}_{14}^1\text{H}_{11} - ^{179}\text{Hf}$ [$\Delta m = 140\,260.3(1.8) \mu\text{u}$] [47]. The results reported here lead to $\Delta m = 140\,251.8(6.5) \mu\text{u}$ being in good agreement. The same is true for the doublet $^{178}\text{Hf}^{35}\text{Cl} - ^{176}\text{Hf}^{37}\text{Cl}$ with the AME-2003 value of $\Delta m = 5\,239.5(1.3) \mu\text{u}$ [51] and the value calculated from the TRIGA-TRAP measurements of $\Delta m = 5\,253.8(12.6) \mu\text{u}$. Other measurements contributing to the AME-2003 adjusted mass values of the hafnium isotopes under investigation are the decays $^{176,177}\text{Lu}(\beta^-)^{176,177}\text{Hf}$ [41,48,49] and $^{179}\text{Ta}(\epsilon)^{179}\text{Hf}$ [50], the mass difference $^{181}\text{Ta}^{35}\text{Cl} - ^{179}\text{Hf}^{37}\text{Cl}$ [52], and the reaction study of $^{180}\text{Hf}(n, \gamma)^{181}\text{Hf}$ [53].

IV. DISCUSSION OF THE RESULTS WITH RESPECT TO NUCLEAR STRUCTURE

The proton-neutron interaction is important in order to understand structural changes in nuclei. It plays a key role, for example, in the onset of collectivity, changes in single-particle energies, magic numbers, and the development of configuration mixing. Double differences of binding energies δV_{pn} , described in Sec. I, are a filter that isolates the average interaction between the last two protons and the last two neutrons. The first experimental studies on δV_{pn} are reported in

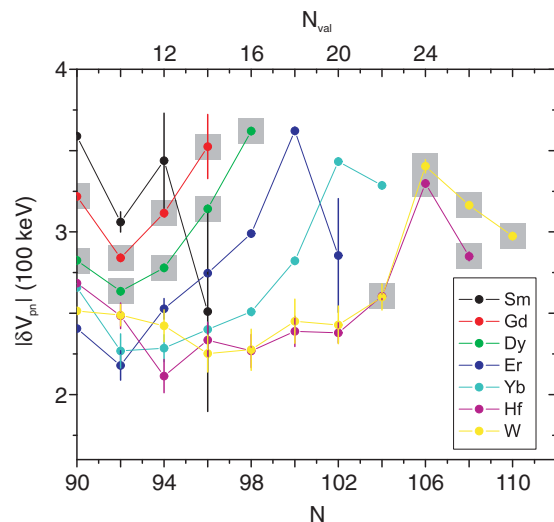


FIG. 6. (Color online) δV_{pn} values as a function of the neutron number N for even-even nuclei in the rare-earth region. In addition, the top axis labels the number of valence neutrons N_{val} . Values where TRIGA-TRAP data contributed are marked with gray boxes. For discussion, see text. Figure is based on Ref. [67].

Refs. [8,9]. In recent years, with the help of the AME 2003 [7] and precise mass measurements, a number of studies on δV_{pn} and its interpretation have been published [10,11,54–62].

The proton-neutron interactions are easily explained in terms of the shell-model orbits occupied by the last nucleons for nonspherical nuclei in the vicinity of closed shells. If the last proton and neutron occupy similar nl_j orbits (with similar n nodes, wavelength, l , and kinetic energies), δV_{pn} is expected to be large. In contrast, if they fill dissimilar orbits, a low δV_{pn} value is expected. These expectations are explained in Ref. [56] in detail, in particular for the ^{208}Pb region (see also Refs. [55,60,62] for the nuclei in the vicinity of closed shells).

The δV_{pn} values in the rare-earth region using the new adjusted mass excesses given in Table I for the case of $^{154-158}\text{Gd}$, ^{160}Gd [$\delta V_{pn}(^{154-160}\text{Gd})$ and $\delta V_{pn}(^{156-164}\text{Dy})$] and $^{176-180}\text{Hf}$ [$\delta V_{pn}(^{176-180}\text{Hf})$ and $\delta V_{pn}(^{178-184}\text{W})$] are presented in Fig. 6.

Large maxima in δV_{pn} occur for light even-even nuclei with $N \simeq Z$, which is explained in terms of Wigner's SU(4) supermultiplet theory in Ref. [11]. Detailed shell-model calculations have also been carried out [11,55,63–65]. Due to the increasing spin-orbit interaction and the Coulomb interaction, this SU(4) symmetry is broken in heavy nuclei (for details, see Refs. [63,64,66]). However, according to Ref. [67], and as seen in Fig. 6, the δV_{pn} values in the rare-earth region nuclei reveal similar systematics for successive nuclei, as in light nuclei, if one considers only the number of valence particles instead of N and Z [although the approach is not an SU(4) symmetry since the protons and neutrons are filling different shells and one only considers the valence nucleons]. The effect seems to result from the higher overlaps of valence proton and neutron wave functions when their respective shells have approximately equal numbers of nucleons ($Z_{\text{val}} = N_{\text{val}}$ and $Z_{\text{val}} \simeq N_{\text{val}}$). It is appropriate to call this a *mini-valence* Wigner effect [67].

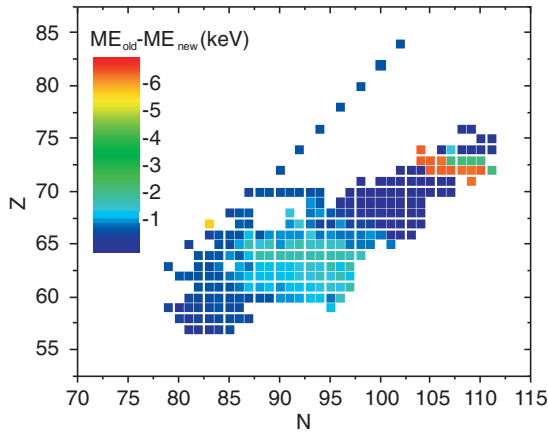


FIG. 7. (Color online) Difference of the adjusted mass excess values in the AME with (ME_{new}) and without (ME_{old}) consideration of the TRIGA-TRAP data. For details, see text.

New mass measurements, of course, are needed for Gd and Dy to see if the rising δV_{pn} values actually maximize at $Z_{\text{val}} \simeq N_{\text{val}}$, and a more precise δV_{pn} value for Sm at $N = 96$ is required as well. Since four binding energies are necessary to extract one δV_{pn} for a given Z and N (see Eq. (2)), ^{158}Sm , ^{156}Nd , and ^{154}Nd masses should be measured precisely for $\delta V_{pn}(\text{Sm})$ at $N = 96$. Moreover, the systematics of these δV_{pn} values suggest specific new high-precision mass measurements for ^{160}Sm and ^{164}Gd .

V. CONCLUSIONS

Direct mass measurements on 15 nuclides in the rare-earth region have been performed. The TRIGA-TRAP results given in Table I provide new anchor points of the mass surface, linking the nuclides under investigation to the atomic-mass standard ^{12}C . Existing data obtained by different experiments have been tested, which are based mainly on nuclear reaction studies but only very little on direct mass measurements. Deviations of up to about 20 keV were found for some of the nuclides under investigation. More high-precision Penning-trap mass measurements are certainly required to identify conflicting input data to the AME. A detailed comparison with the results of such reaction experiments did not show any significant discrepancy, yet. It has to be stressed again that some effort has been made to ensure the accuracy of the TRIGA-TRAP results reported here using the results of carbon-cluster measurements, as well as the results of other

Penning-trap mass spectrometers for certain isotopes as a comparison.

The implementation of the TRIGA-TRAP data into the AME shifted the literature values of the nuclides in the rare-earth region by a few keV, as shown in Table I. It should be mentioned that the complex network behind the AME adjustment, which is formed by the different types of measurements available for mass determination (direct measurements, reactions, decays), causes a shift of a complete portion of the mass surface and not only of the nuclides under investigation. Figure 7 shows the comparison between the mass excess values just before the TRIGA-TRAP data was implemented into the adjustment, ME_{old} , and after it was implemented, ME_{new} . The values ME_{old} already contain results of other measurements that have been performed between 2003 and 2010. More nuclides in the rare-earth region will be investigated to provide further input data to the AME and to manifest the trend of the mass-surface shift in this region.

However, since the energy scale on which nuclear structure effects appear is at least one order of magnitude larger, the shift of the mass surface observed within this work does not require a new interpretation of the nuclear structure in the rare-earth region. The TRIGA-TRAP data linking most of the nuclides investigated for the first time directly to the atomic-mass standard is an important confirmation of the evolution of S_{2n} and δV_{pn} in the rare-earth region. Possibly, the systematics in $\delta V_{pn}^{\text{ee}}$ can be interpreted by a mini-valence Wigner effect, which is similar to light $N \simeq Z$ nuclei, just about an order of magnitude less pronounced. In order to draw further conclusions, masses of certain nuclides, which are presently not known experimentally, have to be measured, such as ^{160}Sm and ^{164}Gd . In addition, the precision of known values has to be improved, e.g., for ^{154}Nd , ^{156}Nd , and ^{158}Sm .

ACKNOWLEDGMENTS

We acknowledge financial support by the Max Planck Society, by the Stiftung Rheinland-Pfalz für Innovation under Contract No. 961-386261/854, by the Bundesministerium für Bildung und Forschung under Contract No. 06MZ91721, and by the US Department of Energy under Grant No. DE-FG02-91ER-40609. Sz.N. acknowledges financial support from the Alliance Program of the Helmholtz Association (HA216/EMMI). R.B.C. thanks the Humboldt Foundation for support. W.N. acknowledges support from the Helmholtz Association (VH-NG 148).

-
- [1] K. Blaum, *Phys. Rep.* **425**, 1 (2006).
 - [2] B. Franzke, H. Geissel, and G. Münzenberg, *Mass Spectrom. Rev.* **27**, 428 (2008).
 - [3] J. Ketelaer *et al.*, *Nucl. Instrum. Methods* **594**, 162 (2008).
 - [4] R. C. Barber, H. E. Duckworth, B. G. Hogg, J. D. Macdougall, W. McLatchie, and P. Van Rookhuyzen, *Phys. Rev. Lett.* **12**, 597 (1964).
 - [5] R. B. Cakirli, R. F. Casten, R. Winkler, K. Blaum, and M. Kowalska, *Phys. Rev. Lett.* **102**, 082501 (2009).
 - [6] A. H. Wapstra, G. Audi, and C. Thibault, *Nucl. Phys. A* **729**, 129 (2003).
 - [7] G. Audi, A. H. Wapstra, and C. Thibault, *Nucl. Phys. A* **729**, 337 (2003).
 - [8] J. D. Garrett and J. Y. Zhang, in *Book of Abstracts*, International Conference on Contemporary Topics in Nuclear Structure Physics, Cocoyoc, Mexico, 1998.
 - [9] J.-Y. Zhang, R. F. Casten, and D. S. Brenner, *Phys. Lett. B* **227**, 1 (1989).

- [10] D. S. Brenner, C. Wesselborg, R. F. Casten, D. D. Warner, and J.-Y. Zhang, *Phys. Lett. B* **243**, 1 (1990).
- [11] P. Van Isacker, D. D. Warner, and D. S. Brenner, *Phys. Rev. Lett.* **74**, 4607 (1995).
- [12] C. Smorra, K. Blaum, K. Eberhardt, M. Eibach, J. Ketelaer, J. Ketter, K. Knuth, and Sz. Nagy, *J. Phys. B* **42**, 154028 (2009).
- [13] M. Kretzschmar, *Eur. J. Phys.* **12**, 240 (1991).
- [14] G. Savard, St. Becker, G. Bollen, H.-J. Kluge, R. B. Moore, Th. Otto, L. Schweikhard, H. Stolzenberg, and U. Wiess, *Phys. Lett. A* **158**, 247 (1991).
- [15] D. Neidherr, K. Blaum, M. Block, R. Ferrer, F. Herfurth, J. Ketelaer, Sz. Nagy, and C. Weber, *Nucl. Instrum. Methods* **266**, 4556 (2008).
- [16] G. Gräff, H. Kalinowsky, and J. Traut, *Z. Phys. A* **297**, 35 (1980).
- [17] M. König, G. Bollen, H.-J. Kluge, T. Otto, and J. Szerypo, *Int. J. Mass Spectrom.* **142**, 95 (1995).
- [18] S. George, K. Blaum, F. Herfurth, A. Herlert, M. Kretzschmar, S. Nagy, S. Schwarz, L. Schweikhard, and C. Yazdijian, *Int. J. Mass Spectrom.* **264**, 110 (2007).
- [19] K. Blaum, G. Bollen, F. Herfurth, A. Kellerbauer, H.-J. Kluge, M. Kuckein, E. Sauvan, C. Scheidenberger, and L. Schweikhard, *Eur. Phys. J. A* **15**, 245 (2002).
- [20] J. Ketelaer, T. Beyer, K. Blaum, M. Block, K. Eberhardt, M. Eibach, F. Herfurth, C. Smorra, and Sz. Nagy, *Eur. Phys. J. D* **58**, 47 (2010).
- [21] K. J. R. Rosman and P. D. P. Taylor, *Pure Appl. Chem.* **70**, 217 (1998).
- [22] M. Kretzschmar, *Int. J. Mass Spectrom.* **264**, 122 (2007).
- [23] A. K. Ray and M. S. Islam, *J. Phys. Condens. Matter* **4**, 4101 (1992).
- [24] S. Rahaman *et al.*, *Int. J. Mass Spectrom.* **251**, 146 (2006).
- [25] A. A. Kwiatkowski *et al.*, *Phys. Rev. C* **80**, 051302(R) (2009).
- [26] D. Beck *et al.*, *Eur. Phys. J. A* **8**, 307 (2000).
- [27] M. Mukherjee *et al.*, *Eur. Phys. J. A* **35**, 31 (2008).
- [28] T. von Egidy, H. G. Börner, and F. Hoyler, *Z. Phys. A* **322**, 669 (1985).
- [29] M. K. Balodis *et al.*, *Nucl. Phys. A* **472**, 445 (1987).
- [30] R. B. Firestone, S. F. Mughabghab, and G. L. Molnár, in *Database of Prompt Gamma Rays from Slow Neutron Capture for Elemental Analysis* (International Atomic Energy Agency, Vienna, Austria, 2007).
- [31] A. M. Spits *et al.*, *JYFL Annu. Rep.*, 95 (1993).
- [32] M. A. Islam, T. J. Kennett, and W. V. Prestwich, *Phys. Rev. C* **25**, 3184 (1982).
- [33] H. H. Schmidt *et al.*, *J. Phys. G* **12**, 411 (1986).
- [34] A. M. Spits and S. J. Robinson, in *Proceedings of the Second International Symposium on Capture Gamma-Ray Spectroscopy and Related Topics* (unpublished).
- [35] C. Granja, S. Pospíšil, J. Kubašta, and S. A. Telezhnikov, *Nucl. Phys. A* **724**, 14 (2003).
- [36] D. C. Kayser and W. H. Johnson Jr., *Phys. Rev. C* **12**, 1054 (1975).
- [37] D. G. Burke and J. M. Balogh, *Can. J. Phys.* **53**, 948 (1975).
- [38] G. R. Dyck, R. J. Ellis, K. S. Sharma, C. A. Lander, M. H. Sidky, R. C. Barber, and H. E. Duckworth, *Phys. Lett. B* **157**, 139 (1985).
- [39] R. C. Barber, R. L. Bishop, J. O. Meredith, F. C. G. Southon, P. Williams, H. E. Duckworth, and P. Van Rookhuyzen, *Can. J. Phys.* **50**, 34 (1972).
- [40] N. Klay *et al.*, *Phys. Rev. C* **44**, 2801 (1991).
- [41] S. Y. Van der Werf, *Zeitschrift für Physik A Hadrons and Nuclei* **259**, 45 (1973).
- [42] F. C. G. Southon, J. O. Meredith, R. C. Barber, and H. E. Duckworth, *Can. J. Phys.* **55**, 383 (1977).
- [43] D. L. Bushnell, D. J. Buss, and R. K. Smither, *Phys. Rev. C* **10**, 2483 (1974).
- [44] A. M. I. Hague *et al.*, *Nucl. Phys. A* **455**, 231 (1986).
- [45] R. Richter *et al.*, *Nucl. Phys. A* **499**, 221 (1989).
- [46] S. T. Boneva, E. V. Vasileva, V. D. Kulik, L. K. Khem, Yu. P. Popov, A. M. Sukhovoi, V. A. Khitrov, and Yu. K. Kholnov, *Izvestiya Akademii Nauk SSSR - Seriya Fizicheskaya* **54**, 1787 (1990).
- [47] J. E. Halverson and W. H. Johnson Jr., *Phys. Rev. C* **20**, 345 (1979).
- [48] P. Marmier and F. Boehm, *Phys. Rev.* **97**, 103 (1955).
- [49] M. S. El-Nesr and E. Bashandy, *Nucl. Phys.* **31**, 128 (1962).
- [50] M. M. Hindi, B. O. Faircloth, R. L. Kozub, K. R. Czerwinski, R.-M. Larimer, E. B. Norman, B. Sur, and I. Žliment, *Phys. Rev. C* **63**, 065502 (2001).
- [51] R. C. Barber, J. W. Barnard, D. A. Burrell, J. O. Meredith, F. C. G. Southon, P. Williams, and H. E. Duckworth, *Can. J. Phys.* **52**, 2386 (1974).
- [52] K. S. Sharma, R. J. Ellis, V. P. Derenchuk, R. C. Barber, and H. E. Duckworth, *Phys. Lett. B* **91**, 211 (1980).
- [53] V. Bondarenko *et al.*, *Nucl. Phys. A* **709**, 3 (2002).
- [54] D. D. Warner, M. A. Bentley, and P. Van Isacker, *Nature Phys.* **2**, 311 (2006).
- [55] D. S. Brenner, R. B. Cakirli, and R. F. Casten, *Phys. Rev. C* **73**, 034315 (2006).
- [56] R. B. Cakirli, D. S. Brenner, R. F. Casten, and E. A. Millman, *Phys. Rev. Lett.* **94**, 092501 (2005).
- [57] M. Stoitsov, R. B. Cakirli, R. F. Casten, W. Nazarewicz, and W. Satula, *Phys. Rev. Lett.* **98**, 132502 (2007).
- [58] D. Neidherr *et al.*, *Phys. Rev. C* **80**, 044323 (2009).
- [59] D. Neidherr *et al.*, *Phys. Rev. Lett.* **102**, 112501 (2009).
- [60] M. Breitenfeldt *et al.*, *Phys. Rev. C* **81**, 034313 (2010).
- [61] R. B. Cakirli and R. F. Casten, *Phys. Rev. Lett.* **96**, 132501 (2006).
- [62] L. Chen *et al.*, *Phys. Rev. Lett.* **102**, 122503 (2009).
- [63] E. Wigner, *Phys. Rev.* **51**, 106 (1937).
- [64] F. Hund, *Zeitschrift für Physik A Hadrons and Nuclei* **105**, 202 (1937).
- [65] P. Vogel and W. E. Ormand, *Phys. Rev. C* **47**, 623 (1993).
- [66] P. T. Nang, *Nucl. Phys. A* **185**, 413 (1972).
- [67] R. B. Cakirli, K. Blaum, and R. F. Casten, *Phys. Rev. C* **82**, 061304(R) (2010).